AD_____

GRANT NUMBER DAMD17-94-J-4469

TITLE: Laser Spin-Exchange Polarized 3He and 129Xe for Diagnostics of Gas-Permeable Media with Nuclear Magnetic Resonance Imaging

PRINCIPAL INVESTIGATOR: Dr. William Happer

CONTRACTING ORGANIZATION: Princeton University
Princeton, NJ 08544

REPORT DATE: November 1996

TYPE OF REPORT: Annual

PREPARED FOR: Commander
U.S. Army Medical Research and Materiel Command
Fort Detrick, Frederick, Maryland 21702-5012

REPORT DOCUMENTATION PAGE

Form Approved
OMB No. 0704-0188

1. AGENCY USE ONLY *(Leave blank)*	2. REPORT DATE	3. REPORT TYPE AND DATES COVERED
	November 1996	Annual (15 Sep 94 - 14 Oct 96)

4. TITLE AND SUBTITLE Laser Spin-Exchange Polarized 3He and 129Xe for Diagnostics of Gas-Permeable Media with Nuclear Magnetic Resonance Imaging

5. FUNDING NUMBERS

DAMD17-94-J-4469

6. AUTHOR(S)

Dr. William Happer

7. PERFORMING ORGANIZATION NAME(S) AND ADDRESS(ES)

Princeton University
Princeton, NJ 08544

8. PERFORMING ORGANIZATION REPORT NUMBER

9. SPONSORING/MONITORING AGENCY NAME(S) AND ADDRESS(ES)

Commander
U.S. Army Medical Research and Materiel Command
Fort Detrick, MD 21702-5012

10. SPONSORING/MONITORING AGENCY REPORT NUMBER

11. SUPPLEMENTARY NOTES

12a. DISTRIBUTION / AVAILABILITY STATEMENT

Approved for public release; distribution unlimited

12b. DISTRIBUTION CODE

13. ABSTRACT *(Maximum 200*

This work involves the development of a new implementation of magnetic resonance imaging using ***laser-polarized*** noble gases. Lasers are used to enhance the MR signal from noble gases such as ^{3}He and ^{129}Xe, making them easily observable in a conventional MRI scanner. Initial experiments have already yielded spectacular magnetic resonance images of the lungs of laboratory animals, and recently the first images of a human subject have been produced. This technology should provide functional information that can be important in evaluating and treating pulmonary embolisms, emphysema, asthma, lung cancer and a wide variety of respiratory problems. Lung function is an important concern for the DoD in many areas, including lung function of aviators at high altitudes, deep sea divers, and chemical warfare environments.

14. SUBJECT TERMS

Magnetic resonance imaging, Polarized 3He and 129Xe

15. NUMBER OF PAGES

25

16. PRICE CODE

17. SECURITY CLASSIFICATION OF REPORT	18. SECURITY CLASSIFICATION OF THIS PAGE	19. SECURITY CLASSIFICATION OF ABSTRACT	20. LIMITATION OF ABSTRACT
Unclassified	Unclassified	Unclassified	Unlimited

FOREWORD

Opinions, interpretations, conclusions and recommendations are those of the author and are not necessarily endorsed by the U.S. Army.

____ Where copyrighted material is quoted, permission has been obtained to use such material.

____ Where material from documents designated for limited distribution is quoted, permission has been obtained to use the material.

____ Citations of commercial organizations and trade names in this report do not constitute an official Department of Army endorsement or approval of the products or services of these organizations.

____ In conducting research using animals, the investigator(s) adhered to the "Guide for the Care and Use of Laboratory Animals," prepared by the Committee on Care and use of Laboratory Animals of the Institute of Laboratory Resources, National Research Council (NIH Publication No. 86-23, Revised 1985).

____ For the protection of human subjects, the investigator(s) adhered to policies of applicable Federal Law 45 CFR 46.

____ In conducting research utilizing recombinant DNA technology, the investigator(s) adhered to current guidelines promulgated by the National Institutes of Health.

____ In the conduct of research utilizing recombinant DNA, the investigator(s) adhered to the NIH Guidelines for Research Involving Recombinant DNA Molecules.

____ In the conduct of research involving hazardous organisms, the investigator(s) adhered to the CDC-NIH Guide for Biosafety in Microbiological and Biomedical Laboratories.

William Happer 12 Nov. 1996

PI - Signature Date

TABLE OF CONTENTS

INTRODUCTION

In its present form, magnetic resonance imaging (MRI) produces images by mapping the hydrogen nuclei in the tissues of the body. However, certain portions of the body, most notably the lungs, have remained difficult to image using conventional MRI. Information about lung function has been even more difficult to obtain with presently available radiological techniques. A new implementation of MRI using *laser-polarized* noble gases has recently been demonstrated[1,2] wherein lasers are used to enhance the MR signal from noble gases such as ^{3}He and ^{129}Xe, making them easily observable in a conventional MRI scanner. Initial experiments have already yielded spectacular magnetic resonance images of the lungs of laboratory animals, and recently the first images of a human subject have been produced. This technology should provide functional information that can be important in evaluating and treating pulmonary embolisms, emphysema, asthma, lung cancer and a wide variety of respiratory problems.

Magnetic resonance imaging with laser-polarized noble gases has been made possible by years of basic physics research in the areas of optical pumping and spin exchange[3,4], largely supported by AFOSR with more recent assistance by ARPA. Optical pumping uses circularly polarized light, most often from a laser, to create a large electron spin polarization in a vapor of rubidium or similar atoms. In a collision with a noble gas atom, the electron spin of the rubidium atom can be transferred to the nuclear spin of a noble-gas atom. Extremely large nuclear polarizations can be obtained on time scales ranging from minutes to a few hours. With Titanium:Sapphire lasers and, more recently, high-power AlGaAs laser diode arrays, it is possible to polarize nuclei in substantial quantities of gas (a few liters at STP). This is enough for use in magnetic resonance imaging.

In magnetic resonance imaging, an image is reconstructed from the radio waves produced by precessing nuclear magnetic moments. For images of human beings, the precessing moments are almost always protons, the nuclei of hydrogen atoms. However, the radio signals from a spin-up nucleus completely cancels the radio signals from a spin-down nucleus, and since the excess of spin-up to spin-down nuclei in normal magnetic resonance imaging is only a few per million. This "thermal polarization" is produced by very large magnetic fields, tens of thousands of times larger than the field of the earth. It is only because of the huge number of protons in living tissue (mostly water) that the radio waves from this part-per-million proton polarization are strong enough to create an image.

By contrast, optical pumping and spin exchange produces noble gas nuclear polarizations of order 1, so that the magnetic resonance signal per noble gas nucleus is one million times larger than the signal per proton in conventional MRI. Thus, even though the density of nuclei in a gas is one thousand times smaller than the density of protons in tissue, the huge increase in polarization more than compensates for the fewer nuclei and very bright images of laser-polarized gas can be obtained.

The first gas images, of the excised lungs of a mouse, were made in 1994 with a few cc's of laser-polarized ^{129}Xe by a team of researchers from Princeton University and the State University of New York at Stony Brook[1]. Further collaboration between Princeton and researchers at Duke University[2] yielded the first images made with laser-polarized ^{3}He; the first lung images[5] of a living guinea pig were reported early in 1995. A team from Princeton and Duke Universities produced the first human lung image[6] at the Duke

Medical School on September 18, 1995. Clinical research is expected to commence in early 1996 at a number of institutions.

MR imaging with laser-polarized noble gases offers a wide variety of possible clinical applications. The large non-equilibrium polarizations allow rapid imaging techniques to be used. Presently, a single "slice" of a human lung can be imaged in much less than one second, so real-time imaging of lung function is possible for the first time. The high resolution offered by the technique and the intrinsic three-dimensional nature of MRI means that areas of compromised lung function can be localized to a much higher degree than presently possible. Current clinical techniques involve the use of inhaled radioactive ^{133}Xe (a gamma emitter) to produce a two-dimensional projection image of the lung with resolutions on the order of 1 cm $\times$ 1cm. The technique is frequently combined with radioactive ^{99}Tc, injected intravenously and imaged in a similar manner. By contrast, initial, fully three dimensional human images using laser-polarized ^{3}He have a resolution of 3mm $\times$ 3mm without any optimization.

While initial experiments have concentrated on imaging in the gas phase, laser-polarized ^{129}Xe offers the further possibility of imaging the blood and tissues as well. Xenon is highly soluble in tissue (especially fatty components) and will dissolve in the blood at levels of order 20% of its concentration in the gas phase. Since the polarization of ^{129}Xe survives 10's of seconds in the blood, imaging with ^{129}Xe of many parts of the body in addition to lungs should be feasible. Dissolved ^{129}Xe has a precession frequency that is easily distinguished from the gas-phase frequency, so gas-phase and tissue images can be recorded separately. Detection of pulmonary emboli (blood clots in the lung), a condition that contributes roughly 200,000 deaths per year in the United States, is envisioned as a procedure which could make excellent use of this type of imaging. Other diagnostic possibilities are almost certain to arise once large-scale clinical research commences. Lung function is an important concern for the DoD in many areas, including lung function of aviators at high altitudes, deep sea divers, and chemical warfare environments.

Thus far, noble gas MRI experiments have made use of commercial MRI scanners which have been retuned to the noble gas precession frequency (a relatively straight-forward and inexpensive task). However, because the signal to noise ratio of the MR signal from laser-polarized noble gases is *independent* of magnetic field strength, imaging with much smaller fields will be possible. A dedicated MRI unit for noble gas imaging would be small, inexpensive, and easily portable.

Although clinical research has yet to begin in earnest, several clinical applications of laser-polarized noble gas MRI are already becoming apparent, and more uses are certain to be uncovered. The production of the polarized noble gases is still grounded in basic physics and this research must continue in order to produce ever growing quantities of polarized noble gases necessitated by medical experiments. Interactions of the noble gas atoms with surfaces, and well as further subtleties of optical pumping and spin exchange efficiency will continue to be explored with the potential for tremendous gains in production capability. Progress in clinical research will depend on further successes in the physics laboratory.

BODY

During the period covered by this report, our research efforts were focused on the applications of laser-polarized ^{3}He and ^{129}Xe in magnetic resonance imaging and on the basic physics that makes this possible. Spectacular ^{3}He images of the lungs of laboratory animals have been acquired in collaborative work with the Center for In Vivo Microscopy at the Duke University Medical School. These were quickly followed by the first images of human lungs, work that is described in more detail in Appendix B. The first ^{129}Xe images of human lungs were acquired in the spring of 1996 by a team of researchers from our group at Princeton and by researchers from the radiology department of the University of Virginia Medical School. The experiments were very successful and they show that because of the high solubility of xenon in human tissue and because the new xenon accumulator described below can make large volumes of ^{129}Xe gas with high spin polarization, imaging of the human brain and of other body parts in addition to the lungs will be possible.

There is rapidly growing international interest in this new technology. Professor Gordon Cates, who is one of the scientific leaders of this ARPA work, gave the kickoff talk at an international workshop on medical imaging with laser-polarized ^{3}He and ^{129}Xe. The workshop was held in Les Houches, France on October 7-11, 1996, and sponsored by the French government. The program for the workshop is attached as Appendix D.

Dr. Bastiaan Driehuys has developed a very effective new system for polarizing large amounts of ^{129}Xe with inexpensive diode laser arrays. The basic idea is to use a high-pressure mixture consisting of a few per cent xenon in a carrier gas that is largely ordinary helium with enough nitrogen to ensure quenching of the laser-excited Rb atoms. The helium pressure-broadens the optical absorption spectrum of the Rb atoms so they can more efficiently absorb light from the diode laser arrays, which typically have a spectral bandwidth of 2 or 3 nm. The helium causes negligible spin depolarization of the Rb atoms, which lose the spin produced by optical pumping primarily in collisions with xenon atoms. As a result of the Rb-Xe collisions, the nuclei of the ^{129}Xe atoms are polarized in two or three minutes.

To accumulate large amounts of spin-polarized ^{129}Xe, the gas mixture flows steadily through an optical pumping chamber. The flow rate is adjusted so a ^{129}Xe atom spends enough time in the pumping chamber to be nearly completely spin-polarized. After flowing out of the chamber, the gas flows into a cold trap, where the xenon condenses to small crystals, resembling ordinary frost or snow, and the helium and nitrogen gas flows through the cold trap without condensing and is vented into the room. A more detailed description of the accumulator is contained in Appendix C.

One of the most important components of this technology is the laser used for spin-exchange optical pumping. We have made good progress understanding the performance of diode laser arrays, which are the preferred technology because of their relatively low cost and promise of reliable performance. We have developed an effective, three-dimensional mapping procedure to determine the electron spin polarization produced by the diode laser arrays in the Rb vapor of the cells. This has allowed us for the first time to quantitatively diagnose the performance of the lasers and to give useful feedback to Opto Power, the company which is supplying and improving the diode laser arrays used in our polarizers.

A fundamental patent "Magnetic Resonance Imaging Using Hyperpolarized Gases,"

Patent Number 5,545,396 was issued to Princeton University and the State University of New York on August 13, 1996 for the work described above. Princeton University has filed additional patents on work supported this DARPA grant, a patent on wall coatings for hyperpolarized gases, a patent on the ^{129}Xe accumulator mentioned above, and a patent on a system to polarize ^{3}He.

Much of the technology developed under this grant is being transferred to the startup company Magnetic Imaging Technologies, Inc. (MITI), located in the Research Triangle area of North Carolina through a licensing agreement with Princeton University. One of the recent new hires of MITI is our former student and postdoctoral research associate, Dr. Bastiaan Driehuys. MITI aims to make magnetic resonance imaging with ^{3}He and ^{129}Xe a commonplace medical diagnostic procedure as soon as possible.

CONCLUSIONS

The aim of this work,as outlined in the **Statement of Work** attached as Appendix A, was to develop as rapidly as possible the capability to produce large amounts of nuclear spin-polarized ^{129}Xe and ^{3}He gas for magnetic resonance imaging of humans and for other applications. This promising new diagnostic method uses conventional magnetic resonance imaging machines, along with laser-polarized ^{129}Xe and ^{3}He gas, to make images of human lungs and other body cavities. Xenon is so soluble in blood and tissue that it will be possible to image other organs like the brain with laser-polarized ^{129}Xe. The research has been very successful, and some of the highlights are:

- The first ^{3}He images of human lungs were obtained in collaboration with the Radiology Department of the Duke University Medical School on September 19, 1995. This work has now been published and a reproduction of the paper is attached as Appendix B.
- Progress has been made in understanding the operation of diode laser arrays for spin-exchange optical pumping of ^{129}Xe and ^{3}He gas. This work, which will soon be ready for publication, has shown that a key problem of current diode laser arrays is their very nonuniform spatial intensity distribution. This problem can be solved by using fiber-coupled arrays, though the laser cost is still an issue. We are working with the laser manufacturer, Opto Power, Inc., to develop a cost effective laser. This is the work proposed in Item 1. of the Statement of Work, "Diode lasers."
- A cryogenic accumulator for laser-polarized ^{129}Xe has been successfully developed to produce the large amounts (liters) of ^{129}Xe needed for diagnostic studies of the human body. The accumulator is very similar to the device proposed in Item 2. of the Statement of Work, "Large-volume source of spin polarized Xe-129." A description of the accumulator has been published, and a copy of the paper is attached as Appendix C.
- The first ^{129}Xe images of a human lung were obtained in collaboration with the Radiology Department of the University of Virginia in the spring of 1996. This kind of experiment was proposed in Item 3. of the Statement of Work, "Magnetic resonance imaging with Xe-129." A preprint of the work, which will submitted for publication in the next few weeks, is available on request from the Principal Investigator.
- Stimulated by our work, the first international workshop on inert gas imaging was held in Les Houches, France during the fall of 1996. The program of this conference is attached as Appendix D.

REFERENCES

1. M.S. Albert, G.D. Cates, B. Driehuys, W. Happer, B. Saam, C.S. Springer and A. Wishnia, "Biological Magnetic Resonance Imaging Using Laser-Polarized ^{129}Xe," Nature, **370**, 199 (1994).
2. H. Middleton, R.D. Black, B. Saam, G.D. Cates, G.P. Cofer, R. Guenther, W. Happer, L.W. Hedllund, G.A. Johnson, K. Juvan, and J. Swartz, "MR Imaging with Hyperpolarized ^{3}He Gas," Mag. Res. Med., **33**, 271 (1995).
3. W. Happer, "Optical Pumping," Rev. Mod. Phys. **44**, 169 (1972).
4. B. Saam, H. Middleton and W. Happer,"Nuclear Relaxation of ^{3}He in the presence of O_2," Phys. Rev. A **52**, 862 (1995).
5. R. D. Black, H. L. Middleton, G. D. Cates, G. P. Cofer, B. Driehuys, L. W. Hedlund, G. A. Johnson, M. D. Shattuck and J. C. Schwartz, "In Vivo ^{3}He MR Images of Guinea Pig Lungs," Radiology **199**, 867 (1996).
6. James R. MacFall, H. Cecil Charles, Robert D. Black, Hunter Middleton, John Swartz, Brian Saam, Bastiaan Driehuys, Christopher Erikson, Gordon D. Cates, W. Happer, G. Allan Johnson, and Carl Ravin, "Technical Note: Potential for MR Imaging of Human Lung Air Spaces with Hyperpolarized ^{3}He," Radiology **200**, 553-558 (1996).
7. B. Driehuys, G. D. Cates, W. Happer, E. Miron and D. K. Walter, "High-Volume Production of Laser-Polarized ^{129}Xe," Applied Physics Letters, **69**, 1668 (1996).

PERSONNEL

The following personnel received full or partial support from the grant during the period covered by this report:

Dr. William Happer, Professor and Principal Investigator

Dr. Gordon Cates, Associate Professor

Dr. Bastiaan Driehuys, Research Associate

Dr. Brian Saam, Research Associate

Dr. Eli Miron, Research Associate

Dr. Andrei Baranga, Research Associate

Ms. Karen Sauer, Graduate Student, PhD candidate

Mr. Dan Walter, Undergraduate Summer Research Student

APPENDIX A

Statement of Work
for ARPA Grant DAMD 17-94-J-4469

Laser Spin-Exchange Polarized ^{3}He and ^{129}Xe
for Diagnostics of Gas-Permeable Media
with Nuclear Magnetic Resonance Imaging

1. **Diode lasers.** We will optimize the design of spin-exchange optical pumping systems for inexpensive diode laser arrays. The important issues are:
   (a) The large spectral linewidth ($\approx$ 2 nm FWHM) of the diode lasers. This makes it necessary to use pumping chambers with high gas pressures, typically several atmospheres or more, to provide enough pressure broadening of the atomic absorption line of the alkali-metal atoms to utilize most of the laser light.
   (b) We will assess the long-term reliability of diode laser arrays for spin-exchange optical pumping. For pumping the vapor of rubidium metal, GaAlAs diode material is needed. In the past, the tendency of the Al to oxidize at the end facets and the related propagation of dark line defects have limited the lifetime of GaAlAs diode lasers. However, major improvements in processing may have resolved these problems. If GaAlAs laser lifetime should be a serious issue, there are good reasons to expect much longer lifetimes from aluminum-free materials like GaSbAs, which can be grown by MOVCD. The operating wavelengths of aluminum-free lasers are too long to pump Rb vapor, but they would be an excellent match for Cs vapor.
2. **Large-volume source of spin polarized Xe-129.** So far, only He-3 is available in sufficient quantities (liters) for magnetic resonance imaging of human lungs. We will develop large volume sources of Xe-129, which is of interest because of its much greater solubility in human tissue than He-3, and because there is an inexhaustible, readily recoverable supply from the atmosphere. The issues we must address here are:
   (a) The spin-exchange and spin destruction cross sections of Xe-129 with alkali-metal atoms are some five orders of magnitude bigger than those for He-3. Other things being equal, this means that Xe-129 can be polarized five orders of magnitude more quickly than He-3. Unfortunately, Xe-129 is also five orders of magnitude more potent in destroying the spin of the alkali-metal atoms than He-3. Selecting the optimum concentration of Xe-129 and other gases in the optical pumping chamber is therefore crucial to allow fast pumping while maintaining adequate spin polarization of the alkali-metal atoms.
   (b) It is more difficult to store spin polarized Xe-129 for long periods of time than is the case for He-3 gas, which can be kept polarized at room temperatures for many hours. We expect to be able to solve this problem by developing deuterated wall coating materials for the cells that contain Xe-129. Work in our laboratory has shown that most of the spin relaxation of Xe-129 is due to interactions with the nuclear magnetic moments of protons of hydrogenated wall materials. Since deuterons have a much smaller magnetic moment than protons, they will cause less spin depolarization.

(c) A very convenient way to maintain spin polarized Xe-129 for long periods of time is to freeze it at liquid nitrogen temperatures or below, where it has completely reproducible spin relaxation times of many hours. We will incorporate cryogenic storage of Xe-129 in our systems.

3. **Magnetic resonance imaging with Xe-129.** Although Xe-129 was used in the very first magnetic resonance images with laser-polarized gases – a mouse lung imaged in a collaboration between our Princeton group and a group at the State University of New York at Stony Brook –the most spectacular recent images have been obtained with He-3, which until now has been available in much larger volumes than Xe-129. With the success of our efforts to make much larger amounts of spin-polarized Xe-129, we will use it to image laboratory animals and perhaps humans. Xenon gas is very soluble in blood, and there is a good possibility that enough Xe-129 will dissolve in the blood to permit magnetic resonance imaging of body tissue. This work will be done in collaboration with enthusiastic research partners at the medical schools of Duke University, the University of Virginia, the University of Texas at San Antonio, and Vanderbilt University.

Human Lung Air Spaces: Potential for MR Imaging with Hyperpolarized He-3[1]

James R. MacFall, PhD
H. Cecil Charles, PhD
Robert D. Black, PhD
Hunter Middleton, PhD
John C. Swartz, PhD
Brian Saam, PhD
Bastiaan Driehuys, PhD
Christopher Erickson, BS
William Happer, PhD
Gordon D. Cates, PhD
G. Allan Johnson, PhD
Carl E. Ravin, MD

Two healthy volunteers who had inhaled approximately 0.75 L of laser-polarized helium-3 gas underwent magnetic resonance imaging at 1.5 T with fast gradient-echo pulse sequences and small flip angles (<10°). Thick-section (20 mm) coronal images, time-course data (30 images collected every 1.8 seconds), and thin-section (6 mm) images were acquired. Subjects were able to breathe the gas (12% polarization) without difficulty. Thick-section images were of good quality and had a signal-to-noise ratio (S/N) of 32:1 near the surface coil and 16:1 farther away. The time images showed regional differences, which indicated potential value for quantitation. High-resolution images showed greater detail and a S/N of approximately 6:1.

Index terms: Lung, MR, 60.12143 • Magnetic resonance (MR), contrast enhancement, 60.12143 • Magnetic resonance (MR), nuclei other than H, 60.12147

Radiology 1996; 200:553–558

CLINICAL magnetic resonance (MR) imaging provides a map of the distribution of hydrogen-1 density in human subjects, mainly in water and fat. Contrast is also provided by the relaxation values (T1, T2) of the H-1 in the tissue and the pulse sequence selected (repetition time, echo time). The success of MR imaging has depended in part on the high concentration of H-1 in tissue. The density of water vapor is very low (on the order of 10^{-4} of the density of water in tissue). MR imaging of the gas spaces in the lungs and the movement of gases (ventilation) has seemed technically unfeasible, since the signal from such sources would also be 10^{-4} of the signal from tissue and thus would be too low to image successfully.

MR imaging of lung gas space is also challenged by poor magnetic-field homogeneity due to many tissue-air interfaces and to the presence of artifacts caused by physiologic motion (cardiac, respiratory). Many MR imaging systems include techniques to reduce or control for motion artifacts. Also, the use of a very short echo time can reduce signal loss due to the magnetic inhomogeneities. The low gas density in lung air spaces, however, has continued to be a problem with conventional MR imaging.

MR imaging generally has low sensitivity because only a very small fraction of H-1 spins are polarized by the applied magnetic field. Typically, spins in a 1.5-T magnetic field will experience only a 10^{-6} polarization (predominance of spins populating the low-energy spin state vs the high-energy spin state).

Dramatically higher polarization values have been achieved with noble gases such as xenon-129 and helium-3 by using optical pumping with lasers, rather than a magnetic field, to create the population difference in the spin states (1,2). With this method, polarizations exceeding 50% can be developed that offer a possible 10^5–10^6 signal enhancement factor. Because the signal is a function of the polarization and the density, the result is a potential factor of 10^2–10^3 signal enhancement. Other considerations related to the difference in the resonant frequency of He-3 or Xe-129 and H-1 can further reduce the potential signal enhancement to between a factor of 10 and 100. Such images have been obtained by using hyperpolarized He-3 in guinea pig lungs (2). In this study, we evaluated the methods and results of obtaining hyperpolarized He-3 images in human lung gas spaces.

Materials and Methods

Gas preparation.—He-3 gas was hyperpolarized by means of spin-exchange collisions with optically pumped rubidium atoms (3), as has been described in detail previously (2). Briefly, research-grade He-3 gas is purchased commercially and transferred to a 150-mL cylindric aluminosilicate glass chamber at 10 atm along with 70 mm Hg of nitrogen-2 and 0.1 g of rubidium metal. The container is heated to 180°C and exposed to 100 W of circularly polarized irradiation from a diode laser array aligned to illuminate the entire volume along the axis of the cylinder. The laser is tuned to the 795-nm D1 resonance of rubidium. The laser induces electronic spin polarization of the rubidium, and this polarization is transferred to the He-3 by means of collisional spin exchange.

The apparatus was aligned with the 10-G fringe field of a 1.5-T imaging magnet. This allowed the polarization buildup to be monitored with a low-field pulsed (nonimaging) nuclear MR detector. After 10–12 hours of optical pumping, polarization levels of between 5% and 15% were achieved. Subsequently the container was cooled to room temperature, which caused most of the rubidium to be deposited on the inner surface of the container. Residual rubidium vapor concentration was 10^{10} atoms per milliliter. The T1 value of the polarized He-3 was at least several hours in the high-pressure glass container.

MR imaging.—Imaging was performed at 1.5 T with a whole-body, commercially available MR imaging unit (Signa, revision 5.3; GE Medical Systems, Milwaukee, Wis) equipped with the spectroscopy accessory. Magnitude images were acquired with a gradient-echo pulse sequence. Normally, such a pulse sequence uses a narrow-band receiver tuned to the Larmor frequency for protons at 1.5 T. The pulse sequence was modified with the manufacturer's research software to use the broad-band receiver that is supplied with its spectroscopic imaging product and to adjust the gradient strengths for the difference in gyromagnetic ratio between He-3 (3,459.31 Hz/G) and H-1 (4,257.26 Hz/G). Thus the same sequence could be used to image at H-1 (63.87-MHz) and He-3 (48.65-MHz) frequencies.

[1]From the Departments of Radiology (J.R.M., H.C.C., R.D.B., G.A.J., C.E.R.) and Physics (J.C.S.), Duke University Medical Center, Bryan Research Bldg, Rm 161C, Research Dr, Durham, NC 27710 ; and the Department of Physics, Princeton University, Princeton, NJ (H.M., B.S., B.D., C.E., W.H., G.D.C.). Received February 12, 1996; revision requested March 13; revision received March 26; accepted April 1. Supported in part by National Institutes of Health grant P41-RR05959, National Science Foundation grant CDR-8622201, Air Force Office of Scientific Research grant F49620-92-J-0211, Advanced Research Projects Agency grant DAMD17-94-J-4469, and Army Research Office DAAH04-94-0204, and by GE Medical Systems. **Address reprint requests to J.R.M.**

A unique feature of imaging with hyperpolarized gas is that there is no need to include spin T1 recovery considerations in the choice of repetition time because there is no recovery of the hyperpolarization in the magnetic field. Thus, a repetition time was chosen that was as short as possible for the readout bandwidth, and an echo time was chosen that was as short as possible with the available gradient strength (1 G/cm, 600-second rise time). Typical operating parameters included coronal orientation, 128×256 matrix, 32-cm field of view, and one signal acquired.

Three examinations were performed. The first, thick-section imaging, was performed with 20-mm section thickness, acquisition of three sections, 14.9/3.3 (repetition time msec/echo time msec), 6° flip angle, and plus or minus 4-kHz bandwidth. Acquisition of the three sections was repeated five times during a 28-second breath hold.

Dynamic imaging was performed with 20-mm section thickness, 7.0/2, 3° flip angle, and plus or minus 16-kHz bandwidth. Thirty images were collected for each of two sections in an interleaved fashion during a period of 54 seconds. The time necessary to obtain an individual image was 0.9 seconds, and the time that elapsed between acquisition of consecutive images for a given section was 1.8 seconds. The subject began shallow breathing after approximately 20 seconds of breath holding while the imaging continued.

Thin-section imaging was performed with a 6-mm section thickness, acquisition of 30 sections, 9.5/3.0, 8° flip angle, and plus or minus 16-kHz bandwidth. The sections were obtained in two passes: The odd-numbered sections were collected in the first pass, and the even-numbered sections were collected in the second pass. The total acquisition time was 36 seconds during a breath hold.

Because the conventional coils for the MR imaging system are tuned for H-1 imaging, an octagonal transmit-receive surface coil 26 cm in diameter (center of conductor) was constructed for the He-3 imaging as shown in Figure 1. The coil was fabricated of 1.25-cm-wide copper foil tape (3M, St Paul, Minn) on a 0.635-cm-thick acrylic substrate with the capacitance (high Q, ceramic capacitors; Dielectric Laboratories, Cazenovia, NJ) distributed on each leg of the structure (eight capacitors total, 120 pF per capacitor). This coil, when loaded with a subject, had a quality factor (Q_L) of 40. The matching network was an element design (4). A standard H-1 frequency preamplifier (GE Medical Systems) with a noise figure of less than 0.5 dB was capacitively retuned for use at the He-3 frequency, and a transmit-receive switch was constructed with use of a lumped element "quarter wave" design (4).

The choice of flip angle in hyperpolarized gas imaging is similar to that in conventional imaging of objects with extremely long T1 values. Because the longitudinal magnetization does not recover to the hyperpolarized level, small flip angles must be used to leave sufficient magnetization for the typically 128 or 256 radio-frequency pulses used in a pulse sequence. Ideally, for a single image, the flip angle would slowly increase during imaging, so that a constant transverse magnetization would be created from the gradually declining longitudinal magnetization. For the present studies, a simpler scheme was used that incorporated a constant radio-frequency flip angle, under the requirement that the transverse magnetization near the end of data acquisition for an image should be reduced by no more than 50% of the initial transverse magnetization. The fraction of magnetization left after n radio-frequency pulses of flip angle α is $\cos^n(\alpha)$; therefore, when n equals 128 pulses and α equals 6° the initial magnetization is reduced by about 50%.

For H-1 imaging, flip angles conventionally have been scaled from the amplitude of the radio-frequency power that corresponds to a 90° flip angle as determined with a preimaging procedure. During this procedure, a 90° pulse should create the maximum signal as long as the repetition time is long enough to allow complete recovery of magnetization. This preimaging procedure cannot be performed in the same manner as a breath hold of polarized He-3, because pulses near 90° remove magnetization that does not recover and hence invalidate the preimaging assumptions. Thus, an approximate determination of the flip angle for the coil was made before human imaging began by using a high-pressure (approximately 10 atm) He-3 nonhyperpolarized phantom, which produces a small but detectable signal, placed at the center of the coil. The coil was loaded with a saline bolus to mimic a human chest. Transmit levels for 90° and 180° pulses were determined with this phantom and were used to calculate the appropriate level for the hyperpolarized gas examinations. Note that because a transmit-receive surface coil was used, the flip-angle calibration refers to the center of the coil. The value of the flip angle away from the center of a circular surface coil falls slowly along the axis for small distances. It reaches 70% of the central value at a distance of one-half the radius and falls to 35% of the value at a distance of 1 radius (5).

Subjects and imaging procedure.—Two healthy male volunteers, aged 38 and 46 years, underwent MR imaging at Duke University Medical Center. The study protocol was approved by the institutional review board, and informed consent was obtained. The subject's heart rate and partial pressure of oxyen were monitored during imaging (Omni-Trak; In Vivo Research, Orlando, Fla). Each subject first underwent conventional H-1 MR imaging so that the region of interest could be located and the general anatomic structures could be visualized. After the MR system was prepared for He-3 imaging, the He-3 gas was passed through a 0.2-m filter (Gelman Sciences, Ann Arbor, Mich) to ensure complete removal of rubidium particles from the gas stream. A gas sample from a similarly polarized cell (obtained without the filter) was analyzed with a residual gas analyzer (Dataquad DAQ 3.2; SpectraMass, Congelton, Cheshire, England) and was found to have no detectable level of rubidium. The filtered gas was collected in a conventional plastic bag (approximately 1.2 L of He-3) to which a plastic tube and hand-operated valve were attached.

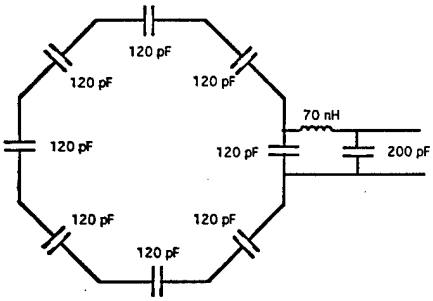

Figure 1. Diagram of the transmit-receive surface coil used for the He-3 imaging. The octagonal section was constructed with 1.25-cm-wide copper foil tape on 0.635-cm-thick acrylic substrate. The coil diameter is 26 cm. *pF* = picofarad, *nH* = nanohenry.

The bag was delivered to the subject in the magnet, and the subject was instructed to open the valve, inhale the gas through the tube, and hold his breath as long as he could. We estimated that approximately 0.75 L of gas actually reached the imaging volume. The subject also had a "squeeze bulb" that actuated a signal audible to the MR operator. For the thick-section and thin-section examinations, the subject actuated the signal when he had completely inhaled the gas. For the dynamic examination, the subject actuated the signal as he began to inhale the gas. Imaging was started when the signal was heard by the operator.

The thick-section and dynamic examinations were performed with one volunteer. The thin-section examination was performed with the second volunteer.

Image analysis.—The signal-to-noise ratio (S/N) of images was calculated for the different examinations by using the display features of the MR system (a cir-

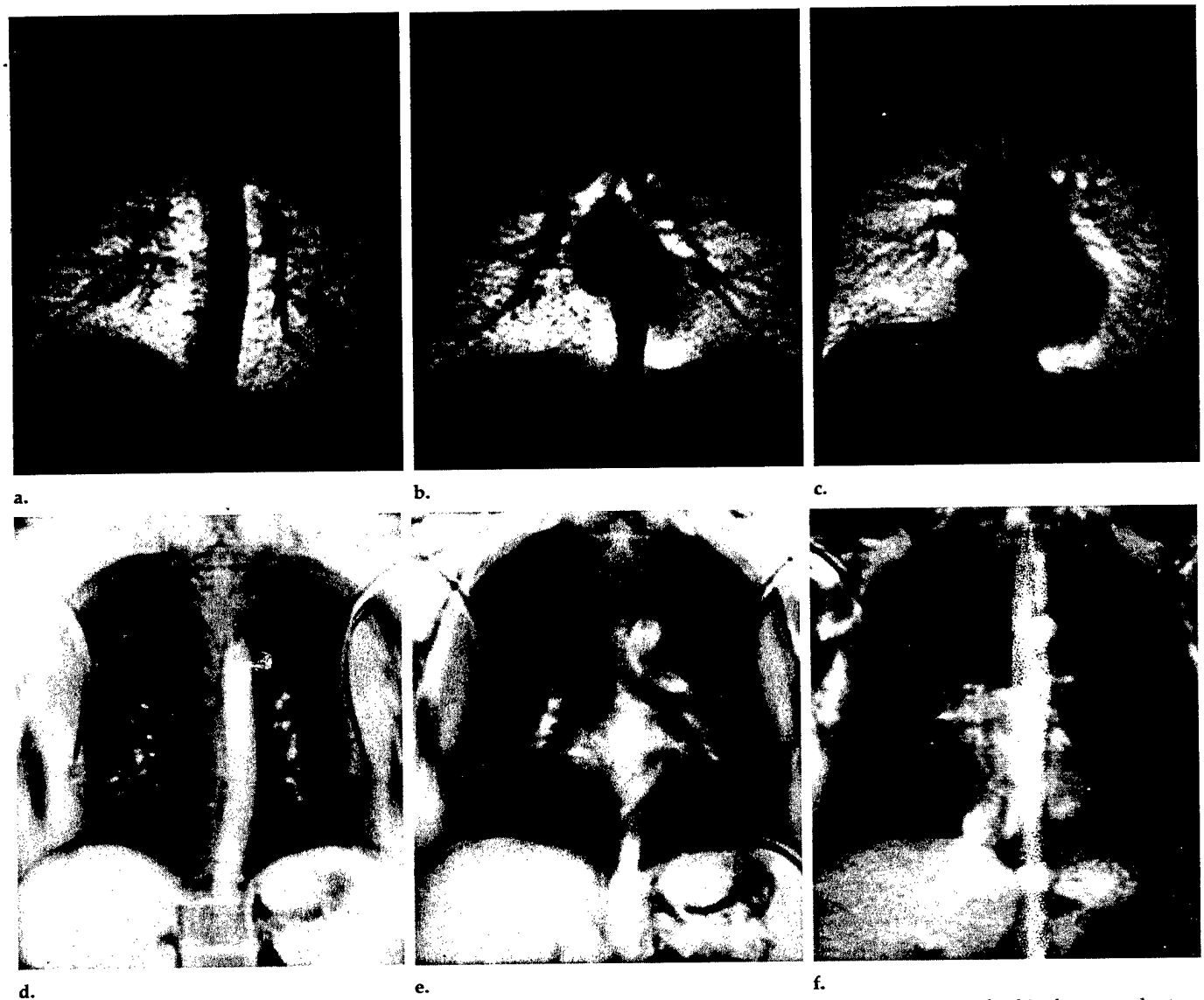

Figure 2. **(a–c)** Thick-section (20 mm) coronal He-3 images and **(d–f)** corresponding H-1 images of the lungs in a healthy human volunteer. The falloff in signal intensity in the apex of the lungs in the He-3 images is due to the position and limited receptivity (26 cm) of the surface coil. The signal intensity on the left and right sides near the edges in **d–f** is an aliasing artifact from the arms and shoulders, which were outside the field of view.

cular cursor superimposed on the image) to define a region of interest. A region of interest of 98 mm^2 was used to determine the average image intensity in a region of the lung field judged to represent "average" features. Also, the standard deviation in a similar region of interest positioned outside the subject and that consisted of noise was used to approximate the image noise (the "air" noise). The S/N was calculated as the ratio of the average region-of-interest signal intensity to the measured air noise. The S/Ns were then corrected by a factor of 0.65 to account for use of air noise, which resulted in underestimation of the true standard deviation (6).

Results

Thick-section imaging.—The subject reported no discomfort during the He-3 breath hold except for a mild tickling sensation at the back of his throat at the end of the breath hold. His Po_2 remained within normal limits for breath holding and his heart rate increased slightly, but both indicators returned to normal after imaging.

The gas processing reached a polarization value of 13%. The signal saturated the preamplifier for the first two repetitions of the sequence and caused strong image artifacts that made the images unusable. Representative thick-section He-3 images corresponding to the third repetition are shown along with the corresponding H-1 images in Figure 2. The S/N for an average-intensity region was on the order of 32:1 in the most anterior image in Figure 2 and decreased to approximately 16:1 in the most posterior image for data acquired in the middle of the acquisition (third repetition).

Dynamic imaging.—The subject reported no discomfort or difficulty in breathing the He-3, and the monitored heart rate and Po_2 changes were unremarkable. Gas polarization for this examination was 5%. A representative sequence of images is shown in Figure 3. The S/N for a representative region on the earliest image was approximately 26:1.

Figure 4 is a graph of image intensity as a function of time (image number) for three regions of interest positioned near the apex, middle, and bottom (near the diaphragm) of the lung, respectively, in the most anterior image series.

Thin-section imaging.—The subject reported no discomfort or ill effects after inhaling the He-3. There were no notable changes in his heart rate or Po_2. A representative image is shown in Figure 5. The gas polarization for this examination was 7%. The S/N for the first-pass

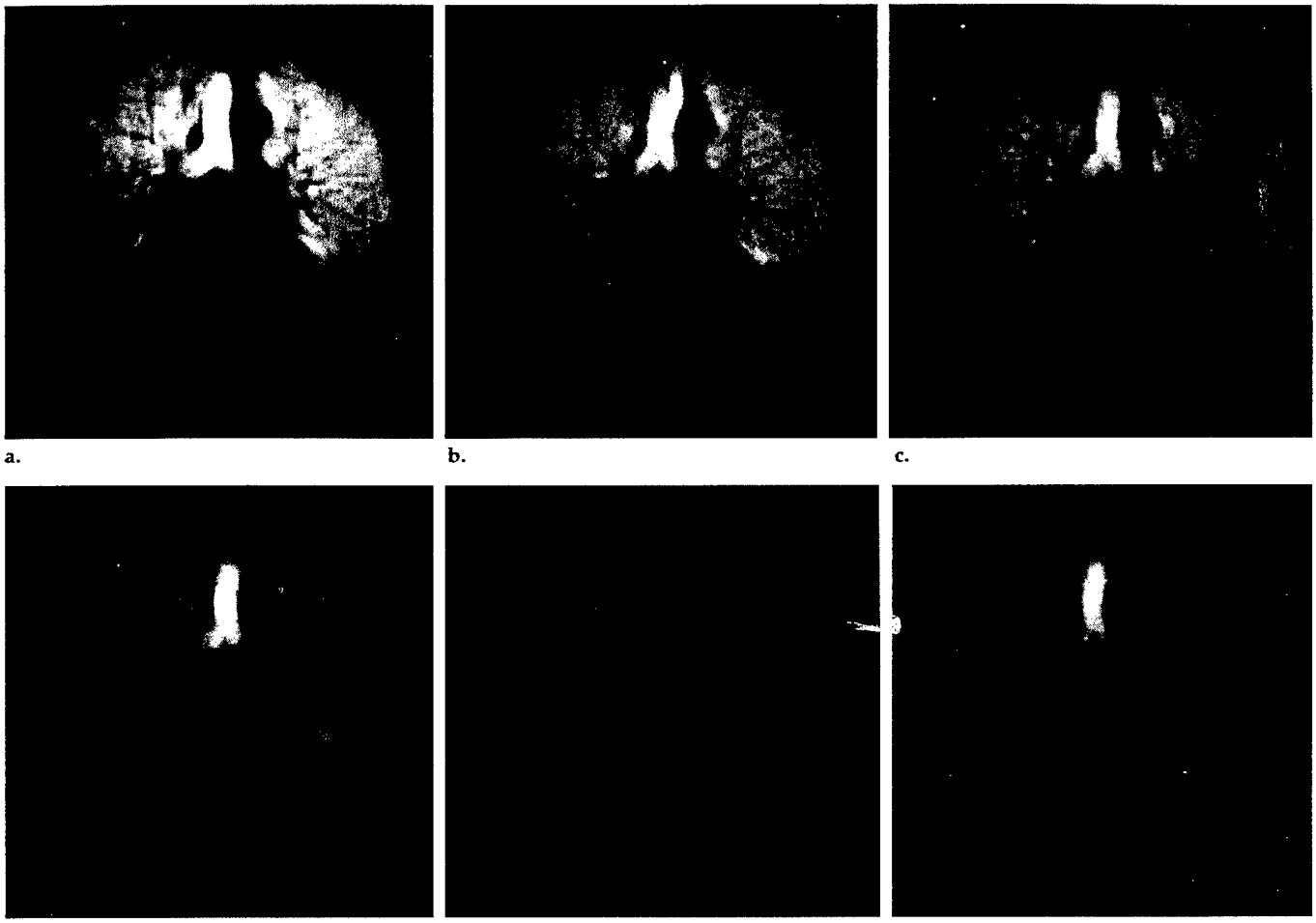

Figure 3. He-3 images selected from a dynamic examination (30 images obtained at 1.8-second intervals) of the distribution of He-3 in the lungs of a healthy volunteer. Acquisition of these images was separated by 3.6 seconds. A reduction in signal intensity due to repetitive imaging of the same section during a breath hold can be seen in **(a–d)** the initial images. The He-3 signal intensity in the trachea **(e)** disappears when the subject begins shallow breathing of room air and then **(f)** reappears during exhalation.

(odd-numbered) images in the anterior region was on the order of 6:1. For the second-pass (even-numbered) sections, the S/N was a factor of nearly one-third less.

Discussion

These results show that very good quality images of the distribution of He-3 in the lungs of a human subject can be obtained with approximately 0.75 L of hyperpolarized He-3 (approximately 8% polarized) and with a minimally modified commercial 1.5-T MR imaging system. The pulse sequence and coils were of conventional design, and their use was well within the capability of most systems and the abilities of most researchers. Typically, multiple acquisitions were made in a given location; therefore, even better S/N could be obtained with use of larger flip angles and a single acquisition.

Thick-section imaging.—The nonuniformity and falloff in signal intensity toward the edges (especially in the apices) was consistent with the position of the surface transmit-receive coil, and the reduction in depth of intensity was also to be expected. The actual anatomic resolution appeared to approach that determined by means of calculated pixel dimension (1.25 × 2.5 mm) as shown by the sharp cutoff of signal intensity at the left and right edges of the lung and at the diaphragm. The indentations into the lungs by the ribs were also remarkable. In addition, the paths of blood vessels appeared as tracks of low intensity, indicating that the He-3 was not taken up by the blood in any large quantity.

The signal intensity that appeared outside the lung in the mediastinal spaces (Fig 2c, center) was an artifact. This artifact was caused by minor saturation of the receiver by the large initial signal at the lowest phase-encoding value in the acquisition and was not thought to represent any penetration of gas into the mediastinal and pleural spaces. The saturation was due to the difficulty of precisely setting the gain of the receiver as described earlier. The subsequent repetitions had a lower signal intensity and no noticeable exterior signal. Figure 2c illustrates this effect at the second repetition of the image. Figure 2a and 2e (fifth repetitions) show that the effect is not present later when

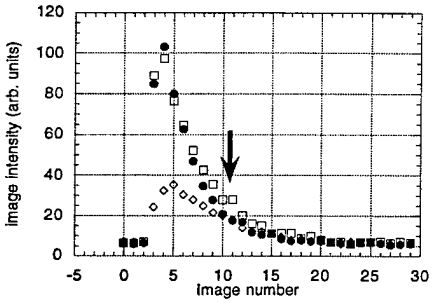

Figure 4. Graph of He-3 signal intensity (arbitrary [*arb.*] units) as a function of image number (0.9 second per image, 1.8-second interval) for three regions of interest (area = 98 mm²) in the lung of a healthy volunteer. The regions of interest are at the apex (□), middle (•), and bottom (◊) of the left lung. The subject began shallow breathing of room air between the 10th and 11th image (arrow).

a. b.

Figure 5. **(a)** Thin-section (6 mm) coronal He-3 image of the lung in a healthy volunteer was obtained at a position through the heart. The falloff in signal intensity toward the bottom of the lung is due to the position and limited receptivity (26 cm) of the surface coil. **(b)** H-1 image of the same region was obtained to help orientation and identification of the anatomic structures.

the signal intensities are decreased. The initial S/N, calculated on the basis of the flip angle prescribed, should be about a factor of 4 higher than that of the third repetition, because each image consumes about half of the available magnetization.

Dynamic imaging.—The coil was positioned more toward the head in this examination than in the thick-section examination. This new position provided better image quality in the apex of the lung but reduced signal intensity near the diaphragm. Use of a reduced flip angle helped preserve the signal intensity throughout the examination, even though the S/N was reduced from the previous examination, because the bandwidth was wider, the polarization was lower, and the flip angle was smaller.

The graph in Figure 4 shows the typical regional dynamics of filling the lungs with gas and exhaling the gas. It also shows the effects of the loss of polarization during the imaging process. Note the delayed peak of the lower part of the lung compared with the other regions. The image intensity was reduced by about 28% after each image was obtained during breath hold and was reduced at a lower rate thereafter. The expectation had been that the signal intensity would be reduced more rapidly during shallow breathing, owing to simple dilution of the He-3 with air; however, the lower-than-expected reduction may be evidence of more complicated gas dynamics that involve inflow of He-3 from unimaged regions of the lung. He-3 from unimaged regions would be at full polarization and would thus slow the loss of image signal intensity. Therefore, although the dynamics appear to be complicated, the fact that the different regions showed different rates of filling and clearance indicates that quantitation of the MR-image time sequences may allow quantitation of regional ventilation.

The series in Figure 3 shows the disappearance of signal intensity in the trachea when the subject began to breathe room air and the reappearance of signal intensity when the subject exhaled. The subject reported that he needed to swallow near the end of the dynamic imaging procedure, and it is interesting to note that a small area of high signal intensity appeared in the region of the stomach, consistent with some gas being transported to the stomach during swallowing.

Thin-section imaging.—The thin-section images exhibited the expected higher anatomic resolution that was seen in the depiction of the cartilage around the trachea and of the dark regions in the lung, corresponding to blood vessels. The images were noisier than the previous examinations, but the value was consistent with use of the larger flip angle, wider bandwidth, and thinner sections. The lower S/N for the second-pass sections was attributed to mixing of the already imaged He-3 gas (depleted magnetization) from the first-pass sections with the gas in the second-pass sections during the 15 seconds between passes; this mixing would lead to approximately a 30% reduction. Additional loss mechanisms likely resulted from a section profile that was somewhat wider than the section spacing. This indicates that sequential rather than alternate section acquisition would provide improved results. Finally, it is possible that the second subject inhaled a smaller quantity of the gas, resulting in lower signal intensity than expected. He also may have loaded the surface coil differently than the first subject, leading to increased noise.

Other technical considerations.—Subjects reported no difficulty breathing the He-3 beyond one mention of dryness in the throat. The gas had no water vapor because of the processing, and so throat dryness was to be expected. Because the use of He-4 is well established in diving mixtures, the safety of He-3, which is chemically identical to He-4, should not be an issue. Subject comfort may be improved by adding water vapor or, for continuous breathing, mixing the He-3 with O_2 that is sufficiently moist before the gas is delivered to the subject.

The use of a transmit-receive surface coil with a large area worked well in this experiment, although the shape and size of the coil could be improved to provide better image uniformity and coverage. The posterior regions in particular suffered S/N loss due to the distance from the surface coil. This loss was a problem in terms of visualization and relative quantitation, because it was difficult to know whether the low signal intensity of a region was due to coil nonuniformity or poor ventilation. Of course, use of a small flip angle helped create a larger region of uniform excitation and reception than would result with use of a large flip angle (the magnetization close to the coil would disappear too rapidly with a large flip angle) (5). In future experiments, we believe development of a larger area "wrap-around" surface coil with a transmit-receive configuration would be valuable.

Radio-frequency power-level calibration also worked well with our procedures but may be too time-consuming for clinical application. If larger quantities of gas were available, preimaging could be automated to occur during a short preliminary hyperpolarized He-3 breath hold, while the steady reduction in signal intensity due to repeated excitations was observed. The rate of reduction would be used to calculate the flip angle. For single-pass imaging, the pulse sequence could include a slowly increasing flip angle calculated to keep the transverse magnetization constant during image acquisition. For dynamic image acquisition, however, use of much smaller flip angles would be necessary to preserve the magnetization throughout multiple acquisitions.

Interpretation of He-3 images.—The images obtained showed that the He-3 gas appeared to rapidly fill all lung spaces and was contained within the lungs, confined by the pleural boundaries of the lung and the trachea. There ap-

peared to be no visible He-3 signal intensity from the blood, the surrounding fat and muscle, or the mediastinal regions. Initially, He-3 was channeled into the lung air spaces in the same manner as a normal air mixture. During a breath hold, the He-3 subsequently moved by convection and diffusion. It is uncertain, however, how well the He-3 was confined to a given region, because He-3 is known to diffuse much more rapidly than air.

The diffusion coefficient of He-3 is on the order of 2.0 cm^2/sec (7); hence, He-3 may move on the order of 1 mm in the 5 msec between phase encoding and readout of the signal. Thus, the ultimate level of spatial resolution may be on the order of 0.5–1.0 mm for He-3. This would still be much higher resolution than is achieved in typical nuclear medicine images. In any case, the images are very promising for thin-section evaluation of ventilation at a segmental level and possibly for quantitation of the gas flow dynamics at a subsegmental level. Much work remains to be done, however, in the evaluation of differences in flow dynamics between He-3 gas-air mixtures and normal air before this technique is clinically applicable.

Although the S/Ns were good, higher values would allow thinner sections to be used. These higher values may be possible if larger quantities of gas are available so that the subject can continuously breathe a mixture of He-3 and O_2. Deep-sea divers routinely breathe a mixture of 16%–20% O_2 with the balance being He-4. Similar mixtures could be prepared for longer term imaging to create high-resolution images with good S/N.

Cost also must be considered in the evaluation of all new imaging methods. Presently, He-3 can be obtained for about $120 per liter. This price is comparable to the usual cost of MR imaging contrast agents and may decrease if demand increases. The source of He-3 is tritium decay; thus its supply depends on the amount of tritium produced. The worldwide supply is limited but is probably sufficient for medical use. It would be possible in a commercial system to recover the He-3 and purify and recycle it, which would extend the supply considerably. The results of this study indicate that lung ventilation images with good resolution can be achieved with use of He-3. Future studies should concentrate on whether such images can contribute important information to the evaluation of lung and airway disease that would justify the cost of MR imaging at the frequencies of both H-1 and He-3. ■

Acknowledgments: We are grateful to Michael J. Souza for construction of the polarization chambers; Steve Suddarth, MS, for help with the preamplifier and coil construction; and Lucy Upchurch for pulse-sequence modifications. We also acknowledge valuable discussions with H. Dirk Sostman, MD, and Vic Tapson, MD.

References

1. Albert M, Cates G, Driehuys B, et al. Biological magnetic resonance imaging using laser-polarized ^{129}Xe. Nature 1994; 370:199–201.
2. Middelton H, Black RD, Saam B, et al. MR imaging with hyperpolarized ^{3}He gas. Magn Reson Med 1995; 33:271–275.
3. Happer W, Miron E, Schaefer S, Schreiber D, Van Wijngaarden W, Zeng A. Polarization of the nuclear spins of noble gas atoms by spin exchange with optically pumped alkali metal atoms. Phys Rev 1984; 29(suppl A):3092–3110.
4. Fukushima E, Roeder S. Experimental pulse NMR: a nuts and bolts approach. Reading, Mass: Addison-Wesley, 1981.
5. Evelhoch J, Crawley M, Ackerman J. Signal-to-noise optimization and observed volume localization with circular surface coils. J Magn Reson 1984; 56:110–124.
6. Kaufman L, Kramer D, Crooks L, Ortendahl D. Measuring signal-to-noise ratios in MR imaging. Radiology 1989; 173:265–267.
7. Barbe R, Leduc M, Laloe F. Resonance magnetique en champ de radiofrequence inhomogene. J Phys 1974; 35:935.

APPENDIX C

High-volume production of laser-polarized ^{129}Xe

B. Driehuys,[a] G. D. Cates, E. Miron, K. Sauer, D. K. Walter, and W. Happer
Department of Physics, Princeton University, Princeton New Jersey 08544

(Received 15 May 1996; accepted for publication 8 July 1996)

A method is described for producing several liters of nuclear spin polarized ^{129}Xe gas via spin exchange with an optically pumped Rb vapor. We use a 140 W AlGaAs laser diode array whose broad spectral output is efficiently absorbed by employing ~10 atm of ^{4}He to pressure broaden the Rb D1 absorption profile. ^{129}Xe is polarized in a continuous gas flow and is then cryogenically accumulated and stored. Extensions of this technique should enable the production of tens of liters of ^{129}Xe with a nuclear spin polarization of order 50%. Production of laser-polarized ^{129}Xe in liter quantities is important for the continued development of magnetic resonance imaging using spin-polarized ^{129}Xe. © *1996 American Institute of Physics.* [S0003-6951(96)01838-4]

The utility of laser-polarized noble gases such as ^{129}Xe and ^{3}He is rapidly becoming apparent in a wide variety of disciplines.[1–5] For example, recent developments in magnetic resonance imaging (MRI) using laser-polarized ^{129}Xe (Refs. 6 and 7) and ^{3}He (Refs. 8–11) have demonstrated the potential for an entirely new medical imaging diagnostic. Initial development of MRI using laser-polarized ^{3}He has progressed rapidly, benefitting from the development of polarized ^{3}He targets for nuclear and medium energy physics experiments,[3,12–15] Until now there has been no comparable technique for production of laser-polarized ^{129}Xe gas in the liter quantities needed for MRI. In this letter we present a method that can be used to produce highly polarized ^{129}Xe in such quantities.

The rate of production of polarized ^{129}Xe via spin exchange with an optically pumped Rb vapor is proportional to the photon current ΔI absorbed by the Rb[16]

$$\frac{d}{dt}\,2\langle K_z\rangle[^{129}\mathrm{Xe}]V=\eta\Delta I, \tag{1}$$

where $[^{129}\mathrm{Xe}]V$ is the number of ^{129}Xe atoms, K_z is the z component of the ^{129}Xe nuclear spin, and η is a measure of the efficiency with which photon angular momentum is converted into nuclear spin angular momentum. The spin-exchange efficiency in the ^{129}Xe–Rb system is $\eta=0.07$;[17] the remaining angular momentum is lost to the rotation of the Rb–Xe pair. Given this efficiency, continuous absorption of 1 W of laser power by the Rb vapor enables the polarization of nearly 40 cm^3 of ^{129}Xe gas per hour.

The dependence of the polarized ^{129}Xe production rate on photon absorption rate points to the need for high laser power. Diode laser arrays, e.g., AlGaAs for the 795 nm D1 line of Rb or InGaAs for the 895 nm D1 line of Cs, are extremely appealing light sources for optical pumping and spin exchange applications. Output powers in excess of 100 W can now be routinely achieved at the 795 nm Rb D1 resonance using stacked arrays. With such high power, low cost and compact structure, these arrays may well replace the traditional Ar^+/Ti:sapphire laser pair for most optical pumping and spin exchange applications.

The primary technical challenge in using diode laser arrays for optical pumping is efficient utilization of their broad spectral output. The spectral distribution of these lasers can be well approximated as Gaussian[15] with a linewidth of 2–3 nm full width at half-maximum (FWHM). One way to permit the Rb vapor to absorb light over such a broad range of wavelengths is to collisionally broaden the Rb D1 absorption profile using a suitable high-pressure buffer gas.[18,19] Several authors have already demonstrated the use of diode laser arrays for spin exchange polarization of ^{3}He.[14,15] By employing ^{3}He densities of order 10 amagat (Ref. 20) (limited only by the structural integrity of the glass pumping cells), the 795 nm Rb absorption resonance is broadened to roughly 0.3 nm FWHM, making it possible to absorb a large fraction of the incident laser power.

Unlike helium, xenon is not well suited as a pressure broadening gas because of its much greater capacity for spin depolarization of the optically pumped Rb.[21] The spin polarization of the Rb vapor during optical pumping is determined by a balance of polarization induced by the absorption of circularly polarized laser light and depolarization caused by collisions of the alkali metal atoms with buffer gas atoms. Optical pumping with a uniform laser profile yields a Rb polarization[22]

$$P_{\mathrm{Rb}}(z)=\frac{\gamma_{\mathrm{op}}(z)}{\gamma_{\mathrm{op}}(z)+\gamma_{\mathrm{sd}}}, \tag{2}$$

where $\gamma_{\mathrm{op}}(z)$ is the optical pumping rate per Rb atom at position z along the pump axis and γ_{sd} is the Rb spin destruction rate

$$\gamma_{\mathrm{sd}}=\sum_i \kappa_{\mathrm{sd}}^i[\mathrm{M}_i], \tag{3}$$

where κ_{sd}^i is the spin-destruction rate coefficient for a given buffer gas, and $[\mathrm{M}_i]$ is its number density. The Rb spin destruction rate due to binary Rb–Xe collisions is $\kappa_{\mathrm{sd}}=5.2\times10^{-15}$ cm^3 s^{-1},[21] more than three orders of magnitude greater than the corresponding spin destruction rate for Rb–^{3}He collisions $\kappa_{\mathrm{sd}}\leqslant(2.3\pm0.2)\times10^{-18}$ cm^3 s^{-1}.[23] To maintain P_{Rb} at sufficiently high levels one needs $\gamma_{\mathrm{op}}\geqslant\gamma_{\mathrm{sd}}$. Although high optical pumping rates can be achieved using diode laser arrays, the laser intensity is depleted within a short distance from the front face of the pump chamber, resulting in a reduction of γ_{op} and a precipitous drop in P_{Rb}.

[a]Electronic mail: driehuys@pupgg.princeton.edu

 0003-6951/96/69(12)/1668/3/$10.00

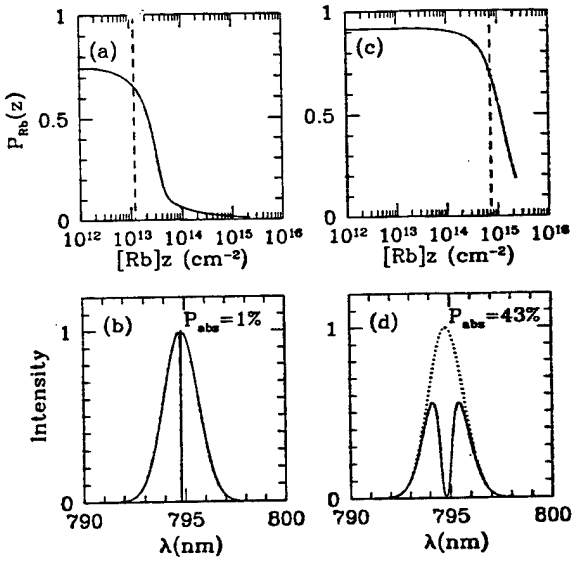

FIG. 1. Comparison of optical pumping with and without ^{4}He pressure broadening. A laser power of 50 W with Gaussian distribution (2 nm FWHM) is assumed incident on a cylindrical cell with an area of 5 cm^2 containing 0.1 amagat of [Xe]. (a) Rapid decrease in Rb polarization with increasing distance z into the cell. (b) Transmitted laser intensity at the dashed line showing narrow absorption of laser light. (c) Using 10 amagat of ^{4}He to pressure broaden the Rb D1 line 60 times more than Rb atoms can be polarized. (d) Transmitted intensity profile shows 43% absorption of the incident laser light.

Figures 1(a) and 1(b) demonstrate optical pumping of Rb in the presence of 0.1 amagat of Xe without the use of an appropriate pressure broadening gas. Equation (2) has been numerically evaluated in a fashion similar to that found in Refs. 13–15 and 23. We have assumed 50 W of collimated diode laser array light (2 nm FWHM) incident on a cylindrical chamber with a front face area of 5 cm^2. Figure 1(a) illustrates the rapid drop in Rb electronic polarization with increasing distance z from the front face of the pump chamber. The dashed line indicates the point at which the volume-average Rb polarization $\langle P_{Rb}\rangle$ has dropped to 90% of the polarization at the front face of the cell $P_{Rb}(0)$. Figure 1(b) shows the remaining laser profile at that point in the cell. Due to the narrow absorption resonance, only 1% of the incident laser intensity is absorbed before the Rb polarization becomes undesirably low. Use of higher pressures of Xe would allow more of the laser light to be absorbed, but would result in unacceptably low alkali spin polarization.

Figures 1(c) and 1(d) demonstrate the use of ~10 amagat of ^{4}He to pressure broaden the Rb D1 resonance so that a much greater fraction of the incident laser light can be absorbed. Due the low spin destruction capacity of ^{4}He compared to Xe, Rb spin relaxation continues to be dominated by collisions with Xe. By again specifying $\langle P_{Rb}\rangle = 0.9P_{Rb}(0)$, we find that the number of Rb atoms that can be polarized is 60 times greater than without ^{4}He broadening, and that 43% of the available laser intensity is absorbed.

The nuclear spin polarization of ^{129}Xe achieved through spin exchange with an optically pumped Rb vapor after a time t_p is

$$P_{Xe}(t_p) = \frac{\gamma_{se}}{\gamma_{se}+\gamma_w}\langle P_{Rb}\rangle(1-e^{-(\gamma_{se}+\gamma_w)t_p}). \quad (4)$$

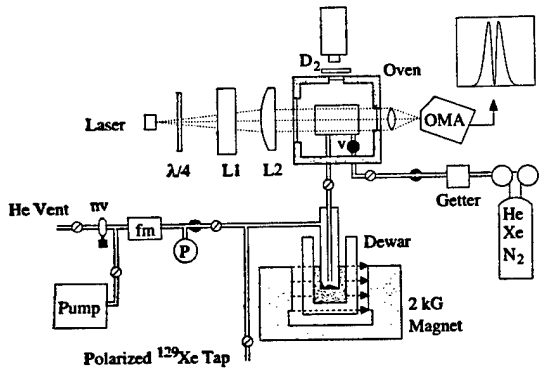

FIG. 2. Schematic of the high-volume ^{129}Xe polarizer. A high-pressure mixture of He, Xe, and N_2 passes through a getter and then through a Rb vaporizer (v) and into the optical pumping chamber. The total gas flow rate is controlled with a needle valve (nv) and measured with a flow meter (fm) while total pressure (P) is monitored. Polarized ^{129}Xe is frozen in a cold finger at 77 K in a 2 kG magnetic field. Once accumulation has stopped, solid Xe is thawed and collected at the polarized ^{129}Xe tap. Optimization of the optical pumping temperature is achieved by monitoring the spectral profile of the light exiting the cell using an optical multichannel analyzer (OMA).

The factor $\gamma_{se}/(\gamma_{se}+\gamma_w)$ results from an equilibrium between the rate of polarization transfer γ_{se} to ^{129}Xe through spin exchange collisions with Rb and the rate of polarization loss γ_w from ^{129}Xe to the cell wall. However, in our system $\gamma_{se} >> \gamma_w$, despite uncoated cell walls.[5] Thus, γ_w can be neglected, giving $P_{Xe}(t_p) \approx \langle P_{Rb}\rangle(1-e^{-\gamma_{se}t_p})$.

The Rb–^{129}Xe spin exchange rate γ_{se} under conditions where He is the dominant third-body gas can be derived from the work of Cates and co-workers[24]

$$\gamma_{se} = [Rb]\left(\langle\sigma_{se}v\rangle + \frac{\kappa_{He}}{[He]}\right), \quad (5)$$

where [Rb] is the number density of Rb atoms, and $\langle\sigma_{se}v\rangle$ is the velocity-averaged binary spin exchange cross section which has been measured to be $\langle\sigma_{se}v\rangle = (3.7\pm0.6)\times10^{-16}$ $cm^3\,s^{-1}$.[24] Spin exchange resulting from the formation of Van der Waals molecules is characterized by κ_{He} which can be estimated from Ref. 24 to be $\kappa_{He} = (1.7\pm0.3)\times10^4$ s^{-1}. At a pumping temperature of 150 °C ([Rb] = 1.04×10^{14} cm^{-1}), which is attainable in our system, the time constant $\tau_{se} = 1/\gamma_{se}$ for spin exchange is only 22 s. Such short spin exchange times make a continuously flowing ^{129}Xe polarization system possible.

Figure 2 shows a schematic of a prototype device that has been constructed to polarize ^{129}Xe in the presence of high-pressure ^{4}He. A gas mixture containing about 98% ^{4}He, 1% Xe, and 1% N_2 (Ref. 25) flows through the optical pumping chamber at roughly 10 amagat. The N_2 serves to collisionally de-excite Rb atoms in the $5P_{1/2}$ state during optical pumping to prevent depolarizing radiation trapping.[26] The gas stream first flows through a zirconium getter[27] which removes H_2O, O_2, CO_2, CO, and other impurities that can react chemically with Rb and result in decreased [Rb]. The gas stream then passes through a hot copper wool mesh coated with Rb metal where it obtains a saturated vapor of Rb. This Rb vaporizer serves to maintain [Rb] against losses resulting from Rb reacting with residual impurities or Rb that leaves the cell in the gas stream. The optical pumping cham-

ber, a cylinder 25 mm in diameter and 80 mm in length, is maintained at a temperature between 130 °C and 150 °C ($3.6\times10^{13}\leq[\mathrm{Rb}]\leq1.0\times10^{14}$ cm^{-3}) depending on the available laser power. The gas flow rate is adjusted using a needle valve so that a ^{129}Xe atom spends several spin-exchange periods in the optical pumping chamber and thus exits highly polarized.

As the gas stream exits the optical pumping chamber, the Rb vapor condenses on the surface of the glass tubing and polarized ^{129}Xe is extracted further downstream by trapping it as a solid in a cold finger. ^{129}Xe retains its polarization during freezing[28] and the strongly temperature-dependent relaxation time of solid ^{129}Xe is about 3 hr at 77 K.[29] The spin lattice relaxation time T_1 of the solid-phase ^{129}Xe constrains the duration of the accumulation. After an accumulation time t_a the remaining polarization of the ^{129}Xe ice is

$$P_{\mathrm{Xe}}(t_a)=P_{\mathrm{Xe}}(0)(T_1/t_a)(1-e^{-t_a/T_1}), \tag{6}$$

where $P_{\mathrm{Xe}}(0)$ is the polarization of the ^{129}Xe exiting the optical pumping chamber. Equation (4) can be substituted for $P_{\mathrm{Xe}}(0)$ and the Xe flow rate F_{Xe} can be related to pumping time t_p through $F_{\mathrm{Xe}}=[\mathrm{Xe}]V_p/t_p$, giving

$$P_{\mathrm{Xe}}(t_a)=\langle P_{\mathrm{Rb}}\rangle(T_1/t_a)(1-e^{-t_a/T_1})\left(1-e^{-\frac{[\mathrm{Xe}]V_p\gamma_{se}}{F_{\mathrm{Xe}}}}\right), \tag{7}$$

where [Xe] is the Xe atom density in the pump chamber and V_p is the volume of the pump chamber. The accumulated equivalent gas volume is $V_{\mathrm{Xe}}=F_{\mathrm{Xe}}t_a/L_0$ where $L_0=2.689\times10^{19}$ atoms/cm^3 is Loschmidt's number.

The final polarization of the ^{129}Xe gas for a desired volume V_{Xe} can be maximized by appropriate choice of gas flow rate and accumulation time. For example, if $T_1=3$ hr ($T=77$ K and $B_0\geq500$ G) and the desired final volume of Xe gas is $V_{\mathrm{Xe}}=500$ cm^3, a ^{129}Xe polarization of 60% can be attained by accumulating for $t_a=1.4$ hr at a flow rate of $F_{\mathrm{Xe}}/L_0=6$ cm^3/min (600 cm^3/min total gas flow rate). Alternatively one could maximize V_{Xe} for a specified polarization level, or maximize the product $V_{\mathrm{Xe}}P_{\mathrm{Xe}}$.

Initial operation of the prototype device has allowed us to produce roughly 1 liter of ^{129}Xe gas with a polarization of 5%. While this represents an order of magnitude increase in previously reported volumes of polarized ^{129}Xe, the polarization level attained was much lower than predicted. The lack of uniformity of our diode array beam profile and the difficulty of collimating the light into the optical pumping cell contribute to this problem. The beam nonuniformity results in regions of low Rb polarization and the lack of collimation results in wasted laser intensity. As evidence of low Rb polarization, a ^{129}Xe polarization of only 22% was observed in the optical pumping chamber when gas flow was stopped. Furthermore, there is some evidence that the relaxation time of the solid ^{129}Xe is not as long as would be predicted from Refs. 28 and 29, perhaps due to the vastly different conditions under which solid Xe is being formed in our system. This would result in lower ^{129}Xe polarizations, especially for the long accumulation time needed to produce 1 liter of gas.

An important aspect of the ^{129}Xe polarization method described here is that it can be readily extended to produce larger quantities of polarized ^{129}Xe without requiring higher laser power. In our present system, the relaxation time of the solid ^{129}Xe constrains the useful accumulation time. By lowering the temperature of the cold finger to 4.2 K one can achieve relaxation times as long as $T_1=12$ days in the solid ^{129}Xe.[29] With such long relaxation times, polarized ^{129}Xe accumulation can continue on time scales of days enabling the production of many liters of gas with a single device. To prevent potential problems of N_2 freezing into the Xe lattice at lower temperatures it may be possible to substitute H_2 as a quenching gas, and condensing at $T=14$ K. Assuming 43% absorption of 50 W of laser light, as in Figure 1(d), and using $\eta=0.07$, 20 liters per day of ^{129}Xe could be polarized.

This work was supported by the AFOSR, ARO, and the Defense Advanced Research Project Agency (DARPA).

[1] G. Navon, Y. Q. Song, T. Room, S. Appelt, E. Taylor, and A. Pines, Science **271**, 1848 (1996).
[2] T. E. Chupp, R. J. Hoare, R. L. Walsworth, and Bo Wu, Phys. Rev. Lett. **72**, 2363 (1994).
[3] P. L. Anthony *et al.*, Phys. Rev. Lett. **71**, 959 (1993).
[4] D. Raftery, H. Long, T. Meersmann, P. J. Grandinetti, L. Reven, and A. Pines, Phys. Rev. Lett. **66**, 584 (1991).
[5] B. Driehuys, G. D. Cates, and W. Happer, Phys. Rev. Lett. **74**, 4043 (1995).
[6] M. S. Albert, G. D. Cates, B. Driehuys, W. Happer, B. Saam, C. S. Springer, and A. Wishnia, Nature **370**, 188 (1994).
[7] M. E. Wagshul, T. M. Button, H. F. Li, Z. Liang, K. Zhong, and A. Wishnia, Magn. Reson. Med. (in press).
[8] H. Middleton, R. D. Black, B. Saam, G. D. Cates, G. P. Cofer, R. Guenther, W. Happer, L. W. Hedllund, G. A. Johnson, K. Juvan, and J. Swartz, Magn. Reson. Med. **33**, 271 (1995).
[9] R. D. Black, H. Middleton, L. W. Hedlund, M. D. Shattuck, G. A. Johnson, J. Swartz, B. Driehuys, G. D. Cates, G. P. Cofer, and W. Happer, Radiology **199**, 867 (1996).
[10] J. R. MacFall, H. C. Charles, R. D. Black, H. Middleton, J. Swartz, B. Saam, B. Driehuys, C. Erickson, W. Happer, G. D. Cates, G. A. Johnson, and C. E. Ravin, Radiology (in press).
[11] M. Ebert, T. Großman, W. Heil, E. Otten, R. Surkau, M. Leduc, P. Bachert, N. V. Knopp, R. Schad, and M. Thelen, Lancet **347**, 1297 (1996).
[12] N. R. Newbury, A. S. Barton, P. Bogorad, G. D. Cates, M. Gatzke, B. Saam, L. Han, R. Holmes, P. A. Souder, J. Xu, and D. Benton, Phys. Rev. Lett. **67**, 3219 (1991); Phys. Rev. Lett. **69**, 391 (1992).
[13] T. E. Chupp, M. E. Wagshul, K. P. Coulter, A. B. McDonald, and W. Happer, Phys. Rev. C **36**, 2244 (1987).
[14] T. E. Chupp and M. E. Wagshul, Phys. Rev. A **40**, 4447 (1989).
[15] W. J. Cummings, O. Hausser, W. Lorenzon, D. R. Swenson, and B. Larson, Phys. Rev. A **51**, 4842 (1995).
[16] N. D. Bhaskar, W. Happer, and T. McClelland, Phys. Rev. Lett. **49**, 25 (1982).
[17] X. Zeng, Z. Wu, T. Call, E. Miron, D. Schreiber, and W. Happer, Phys. Rev. A **31**, 260 (1985).
[18] S.-Y. Ch'en and M. Takeo, Rev. Mod. Phys. **29**, 20 (1967).
[19] A. Gallagher, Phys. Rev. A **157**, 68 (1967); **163**, 206 (1967).
[20] 1 amagat $=2.689\times10^{19}$ atoms/cm^3 (Loschmidt's number), the density of an ideal gas at 273 K and 1 atm.
[21] M. A. Bouchiat, J. Brossel, and L. C. Pottier, J. Chem. Phys. **56**, 3703 (1972).
[22] W. Happer and W. A. VanWijngaarden, Hyperfine Intact. **38**, 435 (1987).
[23] M. E. Wagshul and T. E. Chupp, Phys. Rev. A **49**, 3854 (1994).
[24] G. D. Cates, R. J. Fitzgerald, A. S. Barton, P. Bogorad, M. Gatzke, N. R. Newbury, and B. Saam, Phys. Rev. A **45**, 4631 (1992).
[25] The He, Xe, N_2 gas mixture was obtained from Scott Specialty Gas Co.
[26] W. Happer, Rev. Mod. Phys. **44**, 169 (1972).
[27] Ultrapure, Inc., nitrogen purifier part No. 00040-VCR-N2.
[28] G. D. Cates, D. R. Benton, M. Gatzke, W. Happer, K. C. Hasson, and N. R. Newbury, Phys. Rev. Lett. **65**, 2591 (1990).
[29] M. Gatzke, G. D. Cates, B. Driehuys, D. Fox, W. Happer, and B. Saam, Phys. Rev. Lett. **70**, 690 (1993).

International Workshop on (as of September 29)

Perspectives of MR Imaging using Polarized Gases

L: Lecture (30+10 minutes); C: Contributed (15+5 minutes); P: Poster (short presentation)

Tuesday, October 8

7 pm: *welcome drink*
8 pm: *dinner*

Wednesday, October 9

8:00-8:45 *breakfast*

9:15 Welcome
9:25-9:50 Michèle Leduc (L): 'Optical pumping of noble gases'
9:50-10:30 Gordon Cates (L): 'Polarizing large quantities of ^{3}He and ^{129}Xe by spin exchange optical pumping'

10:30-11:00 *coffee break*

11:00-11:40 Werner Heil (L): 'Optical pumping of metastable ^{3}He: a highly efficient method to produce large quantities of spin polarized ^{3}He'
11:40-12:20 Hubert Ducou-le-Pointe (L): 'Medical imaging modalities: an overview'

12:30 *lunch*

15:00-15:40 Mitchell Albert (L): 'Biomedical applications of hyperpolarized ^{129}Xe (HypX) MRI'
15:40-16:10 Norbert Weiler (L): 'Distribution of pulmonary ventilation and perfusion'

16:10-16:40 *coffee break*

16:40-17:00 Michèle Leduc (C): 'High nuclear polarization in ^{3}He and ^{3}He-^{4}He gas mixtures by optical pumping with a 1083 nm laser diode'
17:00-17:10 Pierre-Jean Nacher (P): 'Optical pumping of metastable ^{129}Xe'
17:10-17:20 Kevin Coulter (P): 'Polarization of ^{129}Xe by laser diode array OP / new lasers'
17:20-17:40 Lesley Rogers (C): 'Complete high power semiconductor laser diode systems for producing spin polarized gases'
17:40-18:00 Nils Carlson (C): 'Narrow-linewidth, high power laser diodes at 1083nm wavelength'

18:00-18:15 *break*

18:15-19:15 Round table discussion - Chair: Ernst Otten
'Optical pumping and laser technology'

19:30 *dinner*

Thursday, October 10

8:00-8:45 *breakfast*

9:00-9:40 Michael Bock (L): '^{3}He MRI: basics and diffusion effects'
9:40-10:20 Luc Darrasse (L): 'The challenge of low-field MRI: a new deal with hyperpolarized gases?'

10:20-10:45 *coffee break*

10:45-11:05 G. Allan Johnson (C): 'Hyperpolarized MRI using projection encoding'
11:05-11:25 Lei Zhao (C): 'Optimal pulse sequences for hyperpolarized ^{129}Xe MRI'
11:25-11:35 Yannick Cremillieux (P): 'Projection-reconstruction imaging with ^{3}He'
11:35-11:45 Frank Kober (P): 'NMR of non-hyperpolarised gas'
11:45-12:15 Reinhard Surkau (C): '^{3}He MRI: provision of polarized ^{3}He and first applications'
12:15-12:25 Thomas Gentile (P): 'Polarized ^{3}He research at NIST'
12:25-12:35 Matthew Rosen (P): 'The Michigan optical pumping and laser polarized Xenon delivery system'

12:30 *lunch*

14:30-14:50 Hans-Ulrich Kauczor (C): 'Imaging of the lungs using ^{3}He MRI: preliminary clinical experience'
14:50-15:10 James R. Brookeman (C): 'MR imaging of the human lungs with hyperpolarized ^{129}Xe gas, and spectroscopy of dissolved phases of ^{129}Xe in the lungs and brain'
15:10-15:30 Matthew Rosen (C): 'Laser polarized ^{129}Xe magnetic resonance imaging and spectroscopy studies: current in vivo results'
15:30-15:50 Scott Swanson (C): 'Brain MRI with laser polarized ^{129}Xe'
15:50-16:00 Angelo Bifone (P): 'Optically enhanced ^{129}Xe and ^{3}He NMR and MRI in cancer research'

16:00-16:30 *coffee break*

16:30-16:50 Geneviève Tastevin (C): 'Dense polarised ^{3}He gas for MRI: metastability-exchange optical pumping and cryogenics'
16:50-17:10 Giorgio Frossati (C): 'Possibility of producing polarised ^{3}He and polarised D_2 by brute-force methods'
17:10-17:30 Masayoshi Tanaka (C): 'Production of nuclear polarized ^{3}He by electron pumping'
17:30-17:50 Hubert Rakhorst (P): 'A production route for enriched ^{129}Xe using Urenco gascentrifuges'

17:50-18:15 *break*

18:15-19:15 Round table discussion - Chair: André Constantinesco
'Perspectives of hyperpolarized gases with respect to functional imaging of respiratory and pulmonary functions'

19:30 *dinner*

After dinner: Round table discussion - Chair: Joseph Hajnal
'Applications to perfusion imaging'

Friday, October 11

8:00-8:45 *breakfast*

9:00-9:45 Alexander Pines (L): 'Enhancement of surface and solution NMR/MRI using laser polarized Xenon'
9:45-10:05 Heinz Jaensch (C): 'Polarized gases: a perspective for surface analysis - status'
10:05-10:25 Ronald Walsworth (C): 'Model of hyperpolarized ^{129}Xe uptake in human tissue'

10:25-11:00 *coffee break*

11:00-11:20 Mitchell Albert (C): 'Temporal dynamics of hyperpolarized ^{129}Xe resonances in living rats'
11:20-11:40 Kevin Coulter (C): 'Uptake of laser polarized ^{129}Xe for NMR and MRI'
11:40-11:50 Giles Santyr (P): 'T_1 relaxation times of ^{129}Xe in tissue homogenates'
11:50-12:10 Mitchell Albert (C): 'Investigation of hyperpolarized ^{129}Xe lifetimes in blood'
12:10-12:30 Ching-Hua Tseng (C): 'Laser-polarized ^{129}Xe spectra in *in vitro* blood and blood derivatives'

12:30 *lunch*

14:00-15:00 Round table discussion - Chair: Robert Black
'Industrial and cost issues'